Talanta 85 (2011) 1246–1252

Contents lists available at ScienceDirect

Talanta

journal homepage: www.elsevier.com/locate/talanta

Synthesis of orientedly bioconjugated core/shell Fe_3O_4@Au magnetic nanoparticles for cell separation

Yi-Ran Cui[a], Chao Hong[b], Ying-Lin Zhou[a], Yue Li[c], Xiao-Ming Gao[b,c], Xin-Xiang Zhang[a,*]

[a] Beijing National Laboratory for Molecular Sciences (BNLMS), Key Laboratory of Biochemistry and Molecular Engineering of Ministry of Education, Institute of Analytical Chemistry, College of Chemistry, Peking University, Beijing 100871, China
[b] Institute of Biology and Medical Sciences, Soochow University, Suzhou 215123, China
[c] Department of Immunology, Peking University Health Science Center, Beijing 100191, China

ARTICLE INFO

Article history:
Received 18 February 2011
Received in revised form 1 May 2011
Accepted 5 May 2011
Available online 12 June 2011

Keywords:
Fe_3O_4/Au magnetic nanoparticles
(Fe_3O_4@Au MNPs)
Oriented immobilization
Antibody
Protein A
Cell separation

ABSTRACT

Orientedly bioconjugated core/shell Fe_3O_4@Au magnetic nanoparticles were synthesized for cell separation. The Fe_3O_4@Au magnetic nanoparticles were synthesized by reducing $HAuCl_4$ on the surfaces of Fe_3O_4 nanoparticles, which were further characterized in detail by TEM, XRD and UV–vis spectra. Anti-CD3 monoclonal antibody was orientedly bioconjugated to the surface of Fe_3O_4@Au nanoparticles through affinity binding between the Fc portion of the antibody and protein A that covalently immobilized on the nanoparticles. The oriented immobilization method was performed to compare its efficiency for cell separation with the non-oriented one, in which the antibody was directly immobilized onto the carboxylated nanoparticle surface. Results showed that the orientedly bioconjugated Fe_3O_4@Au MNPs successfully pulled down $CD3^+$ T cells from the whole splenocytes with high efficiency of up to 98.4%, showing a more effective cell-capture nanostructure than that obtained by non-oriented strategy. This developed strategy for the synthesis and oriented bioconjugation of Fe_3O_4@Au MNPs provides an efficient tool for cell separation, and may be further applied to various fields of bioanalytical chemistry for diagnosis, affinity extraction and biosensor.

1. Introduction

During the past few decades, core/shell magnetic nanoparticles (MNPs) have attracted considerable attention due to their ever-increasing applications in biology and medicine, such as biomolecule purification [1], target delivery [2,3], magnetic resonance imaging [4], and biosensing [5–7]. A considerable number of core/shell magnetic nanoparticles were synthesized, which were commonly composed of the Fe_3O_4 magnetic core and chemically modifiable shell, such as Au [8–10], SiO_2 [11,12], Al_2O_3 [13], polystyrene (PS) [14], poly(methacrylate-divinylbenzene) (PMA-DVB) [15] etc. Among them, gold has been considered as one of the best materials for the shell due to its advantages in magnetic property maintenance for the Fe_3O_4 core [16], reliable chemical stability [17], biocompatibility [18], and versatility in surface modification [19].

Various technologies were developed to synthesize Fe_3O_4@Au MNPs, including co-precipitation [16,19,20], hydrothermal method [2,21] and thermal decomposition [22,23]. And Fe_3O_4@Au MNPs with different nanostructures, such as "dumbbell-like" [24] and "nano-pearl-necklaces" [25] were also reported. Nevertheless, most of the researches focused on the preparation of Fe_3O_4@Au MNPs and the formation mechanism of the nanostructures, and only a limited number of literatures reported their bioconjugation strategy and practical application. Moreover, further modification and application of the synthesized Fe_3O_4@Au MNPs were limited in many of the synthesis strategies, because of their complicated manipulation, poor hydrophilicity and high cost. For example, hydrophobic Fe_3O_4@Au MNPs with high monodispersity can be synthesized by the thermal decomposition technology [10], but a complicated "phase transfer" step was recommended to make Fe_3O_4@Au MNPs aqueously soluble before further bioconjugation [26]. Although a facile strategy was reported to synthesize water-soluble Fe_3O_4@Au MNPs from hydrophobic ones with the help of cetyltrimethylammonium bromide (CTAB) as the surfactant [9], the residual surfactant capped on the particle surface may hinder the subsequent chemical modification of the nanoparticles. Accordingly, methods for synthesizing hydrophilic Fe_3O_4@Au MNPs with low cost, simple manipulation and easy bioconjugation are highly desirable to improve their applications in bioanalytical chemistry and other fields.

The bioconjugation of Fe_3O_4@Au MNPs enables them as carriers of various biomolecules such as DNA, antibody and enzyme, which therefore can be used as biorelated functional materials in

* Corresponding author. Tel.: +86 10 62754680; fax: +86 10 62754680.
E-mail address: zxx@pku.edu.cn (X.-X. Zhang).

0039-9140/$ – see front matter © 2011 Elsevier B.V. All rights reserved.
doi:10.1016/j.talanta.2011.05.010

bioanalytical chemistry, such as affinity extraction [20] and biosensor [27]. The positively charged protein (e.g. antibody and enzyme) can be immobilized to the surface of Fe_3O_4@Au MNPs via physical adsorption [28], but the stability of the adsorbed protein may be a challenge when applied in complex biological samples. Although this problem could be solved by covalently immobilizing the antibody onto Fe_3O_4@Au MNPs coated with a protein-coupling agent [26], accessibility of the antigen to the binding sites may be sterically hindered because the antibody was randomly immobilized and the length of the intermediate linker was relatively short. In our previous work, half-IgG of anti-epitestosterone (17α-hydroxy-4-androsten-3-one, abbreviated as "ET") monoclonal antibodies were immobilized onto Fe_3O_4@Au MNPs through Au-S bindings and successfully applied for pseudo-homogeneous immunoextraction [20], but the preparation of half-IgG from anti-ET mAbs was complicated and time consuming. Therefore, an efficient, economic and simple method for nanoparticle bioconjugation needs to be developed.

To optimize the process of antibody immobilization onto MALDI gold targets, Neubert et al. successfully increased coupling efficiency of antibody and antigen by covalently immobilizing protein G as an Fc receptor for the purpose of orienting the antibody [29]. In this regard, protein A, which was also a well known Fc receptor with commercial abundance [30], would be a promising linker for orientedly immobilizing antibody onto Fe_3O_4@Au MNPs surface. As far as we know, there are no reports describing the potential benefits of using protein A as Fc receptor to orientedly immobilizing antibody on Fe_3O_4@Au MNPs surface to improve the recognition efficiency of antigen. Indeed, it is of interest to assess whether Fe_3O_4@Au MNPs conjugated with oriented antibody would offer substantive advantages over those directly covalently attaching the antibody on their surface.

In this work, a simple, efficient and low cost strategy was developed for orientedly immobilizing antibody onto Fe_3O_4@Au MNPs surface using protein A as an intermediate linker. The hydrophilic Fe_3O_4@Au MNPs were synthesized by the reduction of $HAuCl_4$ onto the surface of Fe_3O_4 magnetic nanoparticles which were prepared by coprecipitation of Fe^{3+} and Fe^{2+} in water. The synthesis and bioconjugation processes of Fe_3O_4@Au MNPs were characterized in detail by TEM, XRD, UV–vis spectra, FT-IR and SDS-PAGE step by step. The depletion of $CD3^+$ T cells from whole splenocytes were carried out using the as synthesized anti-CD3 mAb conjugated Fe_3O_4@Au MNPs. High efficiency (up to 98.4%) can be achieved in depleting $CD3^+$ T cells from various amount of mouse splenocytes (from 1×10^6 to 9×10^6), yielding a more efficient cell-capture nanostructure than that using nanoparticles coated with directly immobilized anti-CD3 mAb in random orientations.

2. Experimental procedures

2.1. Reagents and materials

16-MHA ($HS(CH_2)_{15}CO_2H$, 90%), protein A and green fluorescent protein (GFP) were purchased from Sigma–Aldrich, *N*-(3-dimethylaminopropyl)-*N*′-(ethylcarbodiimide) hydrochloride (EDAC, 98%), *N*-hydroxysuccinimide (NHS, 98%) were purchased from Alfa Aesar. Ferrous chloride tetrahydrate ($FeCl_2{\cdot}4H_2O$) was provided by Shantou Xiling Chemical Factory (Shantou, China). Ferric chloride hexahydrate ($FeCl_3{\cdot}6H_2O$) was purchased from Sinopharm Chemical Reagent Co. Ltd. (Shanghai, China). Hydroxylammonium chloride ($NH_2OH{\cdot}HCl$) sodium citrate dyhydrate ($Na_3C_6H_5O_7{\cdot}2H_2O$) and tetramethylammonium hydroxide (TMAOH) aqueous solution (10%, w/v) was purchased from Beijing Chemicals (Beijing, China). Chloroauric acid tetrahydrate ($HAuCl_4{\cdot}4H_2O$) was provided by Shenyang Research Institute of Nonferrous Metals (Shenyang, China). Anti-CD3 mAb was obtained from immunized mice and purified by 3-step $(NH_4)_2SO_4$ precipitation method. Pure water from a Milli-Q water purification system (Millipore, Molsheim, France) was used throughout the study. Other reagents were of analytical grade and were used without further purification.

2.2. Instrumentations

TEM characterization was performed using a JEM-2100 TEM (JEOL, Japan). XRD patterns were recorded on a D/MAX 2400 X-ray diffractometer (Rigaku, Japan). FT-IR spectra were taken on a Nicolet iNIO MX infrared Fourier transform spectrometer (Thermo Fisher, USA). UV–vis spectra were recorded on a Lambda 35 UV–vis spectrophotometer (Perkin Elmer, USA). Zeta potential measurements were performed using a Brookhaven ZetaPlus instrument. Fluorescent image was obtained on a DM 1L microscope (Leica, Germany), coupled with an $iXon^{EM}$ + CCD (Andor Technology plc, Britain). The flow cytometry analysis was performed on a BD FACSCalibur System (BD Biosciences, USA). Magnetic properties were analyzed using a 2900-04C magnetometer (PMC, USA). NdFeB magnet (~4000 G) was obtained from commercial source.

2.3. Buffers and stock solutions

The 0.01 M PBS buffer (pH 7.4) was prepared by dissolving 8.0 g of NaCl, 2.9 g of $Na_2HPO_4{\cdot}12H_2O$, 0.2 g of KH_2PO_4, and 0.2 g of KCl to 1 L of deionized water. Separation buffer was 0.01 M PBS containing 0.1% (w/v) BSA and 0.05% (v/v) Tween-20.

2.4. The synthesis of Fe_3O_4@Au MNPs

Fe_3O_4@Au MNPs were prepared according to previous reported methods with minor modifications [19,20]. 25 mL aqueous solution containing 0.8 M $FeCl_3$, 0.4 M $FeCl_2$, 40 mM HCl was added dropwise into 250 mL of 1.5 M NaOH solution under vigorous stirring using a nonmagnetic stirrer. Black Fe_3O_4 MNPs formed immediately, which were separated by a NdFeB magnet and washed by 200 mL deionized water 3 times. The Fe_3O_4 MNPs were collected by centrifugation at 9000 rpm for 15 min, and resuspended in 100 mL deionized water to obtain 0.1 M Fe_3O_4 suspension, which was stored at 4 °C for further use.

Then $HAuCl_4$ was gradually reduced by NH_2OH in Fe_3O_4 suspension to form a thin gold shell on the magnetite nanoparticle surface. 5 mL 0.1 M Fe_3O_4 suspension was added into 75 mL 0.01 M TMAOH aqueous solution, and the mixture was sonicated for 5 min. Then the mixture was heated to 80 °C under vigorous stirring. 40 mL 0.1% (w/v) $HAuCl_4$ solution was added into the mixture drop by drop, after which 100 mL 15 mM sodium citrate solution was added dropwise. The colour of the mixture changed from black to reddish brown gradually. After heated for additional 1 h, the reaction mixture was cooled to room temperature, and the formed Fe_3O_4@Au MNPs were collected by a magnet, followed by 2 wash-centrifugation cycles with 50 mL deionized water and 2 wash-centrifugation cycles with 50 mL ethanol. The Fe_3O_4@Au MNPs were isolated by centrifugation at 9000 rpm for 15 min and dried at 70 °C in a vacuum oven for 1 h.

2.5. Carboxylation of Fe_3O_4@Au MNPs

16-MHA was self-assembled on Fe_3O_4@Au MNPs surface by the well known Au–S chemistry. 25 mg Fe_3O_4@Au MNPs were suspended in 10 mL ethanol solution of 20 mM 16-MHA, and sonicated for 48 h. The carboxylated nanoparticles were washed 3 times with ethanol and resuspended in 12.5 mL ethanol to obtain 2 mg/mL car-

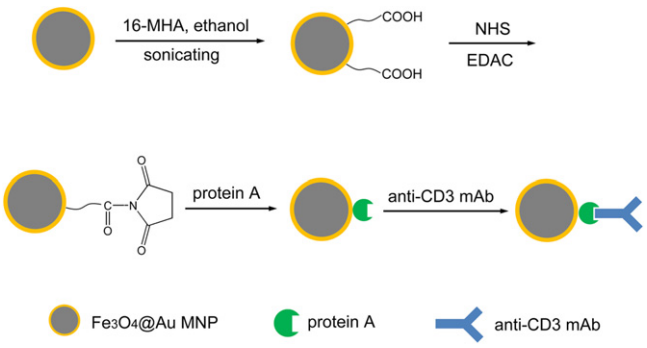

Fig. 1. Illustration of the oriented immobilization of anti-CD3 mAb on Fe_3O_4@Au MNPs.

boxylated Fe_3O_4@Au MNPs suspension, which was stored at 4 °C for further use.

2.6. Anti-CD3 mAb conjugation to Fe_3O_4@Au MNPs

The procedure for oriented anti-CD3 mAb immobilization was described in Fig. 1. 500 μL 2 mg/mL carboxylated Fe_3O_4@Au MNPs were added into an Eppendorf tube, which was placed on a magnet, and the carboxylated Fe_3O_4@Au MNPs were isolated by the magnet in 5 min. The supernatant was discarded and the separated carboxylated Fe_3O_4@Au MNPs were resuspended in 1 mL aqeous solution containing 20 mg/mL EDAC and 10 mg/mL NHS followed by sonicating for 1 h. The active MNPs were collected by a magnet and resuspended in 1 mL PBS containing 150 μg/mL protein A, which was gently shaken at 4 °C overnight. The protein A coated MNPs were separated by a magnet, and the concentration of protein A in the supernatant was analyzed by Bradford assay [31]. And the amount of protein A immobilized on 1 mg Fe_3O_4@Au MNPs was estimated by comparing its concentration before and after the coupling reaction. Then the protein A immobilized Fe_3O_4@Au MNPs were resuspended in 1 mL PBS containing 100 μg/mL anti-CD3 mAb, which was immobilized on MNPs with protein A as the intermediate linker after gently shaking overnight at 4 °C. The amount of immobilized anti-CD3 mAb was tested with the method similar to that of the immobilized protein A. The anti-CD3 mAb modified MNPs were washed 3 times by 1 mL separation buffer and resuspended in 1 mL separation buffer, stored at 4 °C for further use.

As a control, non-oriented anti-CD3 mAb was directly conjugated to the carboxylated Fe_3O_4@Au MNPs. After reaction with NHS/EDAC, the active carboxylated Fe_3O_4@Au MNPs were incubated with 1 mL PBS containing 150 μg/mL anti-CD3 mAb at 4 °C overnight. Then they were washed 3 times and stored at 4 °C for the control experiment.

2.7. SDS-PAGE analysis of orientedly immobilized anti-CD3 mAb on the Fe_3O_4@Au MNPs

250 μL stored Fe_3O_4@Au MNPs immobilized with oriented anti-CD3 mAb were washed with 100 μL PBS for 3 times, and resuspended in 25 μL loading buffer, which was heated in boiling water for 5 min. The linkage between anti-CD3 mAb and protein A was broken, and the immobilized anti-CD3 mAb that released

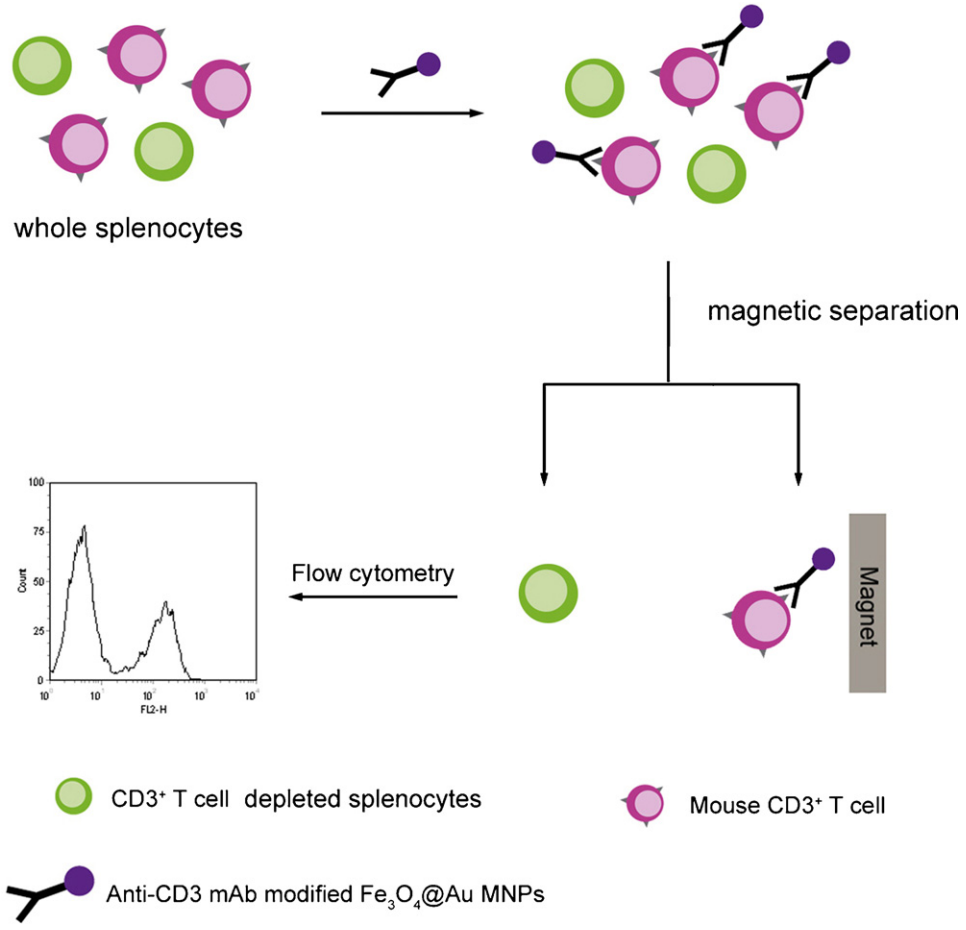

Fig. 2. Procedure of magnetic cell separation for whole splenocytes of mouse using anti-CD3 mAb modified Fe_3O_4@Au MNPs.

from Fe_3O_4@Au MNPs was extracted by the loading buffer. The Fe_3O_4@Au MNPs were isolated by a magnet and discarded. Then 10 μL anti-CD3 mAb extraction was loaded for SDS-PAGE analysis which was performed as reported [32].

2.8. Magnetic cell separation

Magnetic cell separation was carried out by using the anti-CD3 mAb modified Fe_3O_4@Au MNPs (Fig. 2). Briefly, 400 μL nanoparticles were mixed with different amount of mouse splenocytes respectively, and gently stirred at 4 °C for 30 min. Then Fe_3O_4@Au MNPs were separated by a magnet. The cell suspension was replaced into another Eppendorf tube and centrifugated. 100 μL phycoerythrin labeled anti-CD3 mAb (PE-CD3 mAb) was incubated with the collected cells for 15 min at room temperature. Cells were then washed twice with separation buffer and analyzed by flow cytometry.

3. Results and discussion

3.1. Synthesis and characterization of Fe_3O_4@Au MNPs

The synthesis of Fe_3O_4@Au MNPs involved two steps: the formation of Fe_3O_4 magnetic core and the coating of gold shell. The magnetite nanoparticle (Fe_3O_4) core was synthesized via coprecipitation method by adding an acidic solution containing Fe^{3+} and Fe^{2+} (with a molar ratio 2:1) into a basic aqueous solution of NaOH. Nitrogen atmosphere was applied in normal synthesis process to avoid ferrous ion oxidation but it was not applied in this work. And a small number of γ-Fe_2O_3 was formed accompanying the formation of Fe_3O_4. Our research showed that no obvious decrease in the magnetic property of the Fe_3O_4 MNPs, which was caused by partial oxidation, was observed (data not shown). In several literatures, Fe_3O_4 MNPs were partially oxidated to γ-Fe_2O_3 by exposed to air for extended periods (≥1 week) [16] or heated in an acidic solution (for example, 0.1 M HNO_3 solution) with the existence of oxygen [16,28,33]. Since pure Fe_3O_4 MNPs were more resistant to Au deposition than were partially oxidated Fe_3O_4 MNPs [16], the partially oxidated magnetic nanoparticles were chosen as the magnetic core in this study.

Because of the particle growth mechanism, the control of the Fe_3O_4 core size distribution was a little difficult in the coprecipitation method compared with the hydrothermal method. There were two steps in the coprecipitation method for Fe_3O_4 MNPs synthesis [34,35]: (a) short burst of nucleation occurs when the concentration of Fe_3O_4 reaches the critical supersaturation; (b) slow growth of the nuclei by diffusion of the Fe^{2+} and Fe^{3+} to the surface of the Fe_3O_4 crystal. And the factors which could influence the size distribution and particle morphology of Fe_3O_4 MNPs include temperature, nature of the salts, Fe^{3+}/Fe^{2+} concentration ratio, injection fluxes, iron and base concentration, oxygen, etc. [35].

Besides the morphology of the Fe_3O_4 core, the formation of the Au shell and the morphology of Fe_3O_4@Au MNPs were largely related with the amount of added $HAuCl_4$ and the reaction temperature. When the reduction of $HAuCl_4$ was performed at room temperature, some of Fe_3O_4 MNPs were coated with thick Au shell, while some of Fe_3O_4 MNPs were still kept uncoated (data not shown), because Au^{3+} was preferentially reduced onto the existing gold shell of Fe_3O_4@Au MNPs due to thermodynamic process in this step, causing asymmetric shell coating on Fe_3O_4 MNPs. While the reaction temperature rose to 80 °C, Au^{3+} was symmetrically reduced on Fe_3O_4 core, and relatively uniform MNPs were obtained, which were confirmed by TEM (Fig. 3). The average diameter of synthesized Fe_3O_4@Au NPs was 14–19 nm.

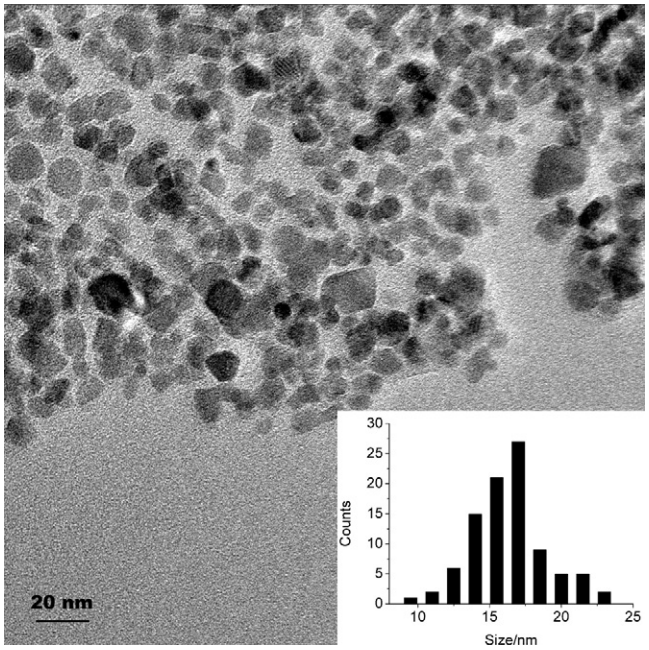

Fig. 3. TEM images of the core/shell Fe_3O_4@Au MNPs. Insets: Histograms of the particle diameters.

Due to the weight contribution from the nonmagnetic Au, the formation of the Au shell resulted in the decrease in the magnetic strength of the core/shell nanoparticles. The different molar ratios of Fe_3O_4 to Au were investigated and a molar ratio of 5:1 had a wonderful performance both in magnetic property maintenance and effective protective coating [19], which was chosen for Fe_3O_4@Au MNPs synthesis in this study. The saturation magnetizations of Fe_3O_4 MNPs and Fe_3O_4@Au MNPs were 29.6 and 15.2 emu/g, respectively (Fig. 4A). Though the magnetic strength of Fe_3O_4@Au NPs decreased after Au shell coating, it was strong enough to allow the separation of Fe_3O_4@Au MNPs by a NdFeB magnet in 2 min (Fig. 4B).

The coated Au shell was confirmed by XRD. The synthesized Fe_3O_4 MNPs and Fe_3O_4@Au MNPs were compared in the XRD spectra (Fig. 5). Fe_3O_4@Au MNPs exhibited diffraction peaks (at $2\theta = 38.2°$, 44.4°, 64.7° and 77.8°), which were indexed to (1 1 1), (2 0 0), (2 2 0) and (3 1 1) planes of gold cubic phase, respectively. At the same time, Fe_3O_4@Au MNPs exhibited all the diffraction peaks of pure Fe_3O_4 MNPs. This information implied that a thin gold shell, which was not thick enough to overlay the Fe_3O_4 diffraction peaks, was successfully coated on the Fe_3O_4 core.

UV–vis absorption of the Fe_3O_4 MNPs and the core/shell Fe_3O_4@Au MNPs showed different absorption properties as shown in Fig. 6. There was no obvious absorption peak exhibited in the spectrum of Fe_3O_4 MNPs, while a peak at 545 nm was found in the spectrum of Fe_3O_4@Au MNPs. In pure Au NPs, the collective oscillations of free electrons, known as the surface Plasmon (SP), cause an absorption peak at 525 nm (Fig. 6c) of the electromagnetic spectrum [16,36]. Clearly, this optical property change in the spectrum of Fe_3O_4@Au MNPs is caused by the Au shell on their surfaces, indicating that Au shell was successfully coated on the Fe_3O_4 MNPs surface. The obtained Fe_3O_4@Au MNPs powder can be well redispersed in water, PBS and ethanol (Fig. S1), and they were negatively charged in water with average zeta potential of −22 mV.

3.2. Bioconjugation of Fe_3O_4@Au MNPs

The coating of Au shell onto the Fe_3O_4 core provides a modifiable surface for the introduction of various groups for protein immobi-

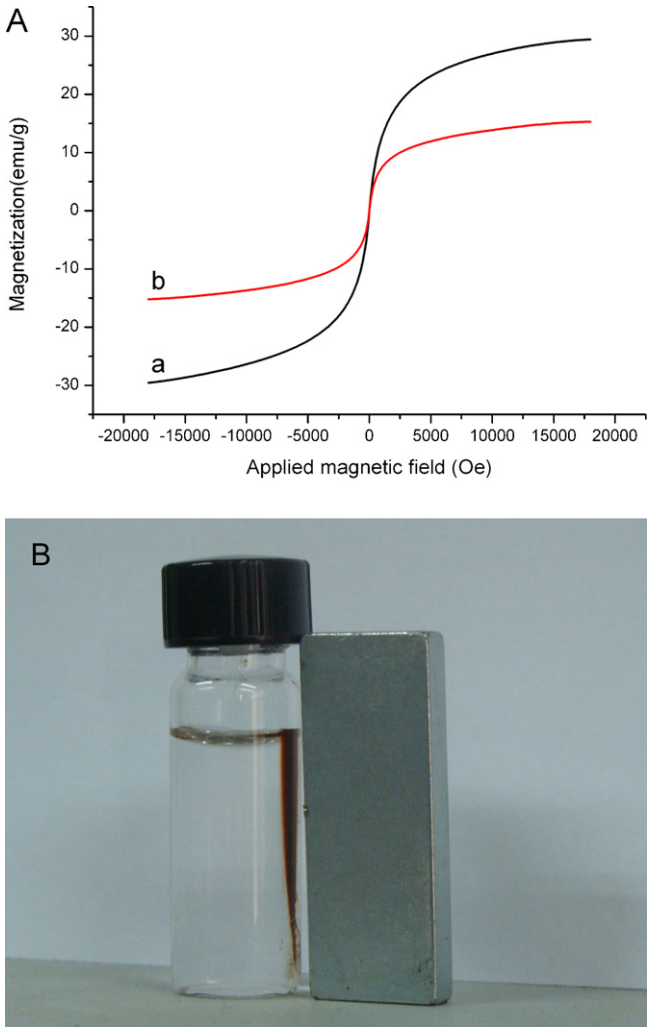

Fig. 4. (A) Magnetization measurements as a function of applied field for pure Fe_3O_4 MNPs (a) and core/shell Fe_3O_4@Au MNPs (b); (B) The Fe_3O_4@Au MNPs can be separated from the suspension by applying a NdFeB magnet.

lization. In this work, 16-MHA was used to modify the surface of the Fe_3O_4@Au MNPs to form self-assembled monolayers with chemically modifiable carboxyl groups via Au-thiol binding. Successful surface modification with 16-MHA was verified by infrared spectroscopic analysis (Fig. 7). For both 16-MHA modified Fe_3O_4@Au MNPs (Fe_3O_4@Au@16-MHA) and pure 16-MHA, asymmetric and symmetric stretching vibrations of the $\nu_a(CH_2)$ and $\nu_s(CH_2)$ of 16-MHA were observed at 2920 and 2850 cm^{-1}, respectively (Fig. 7b and c). The most prominent feature of the carboxylic acid-terminated 16-MHA SAMS was the carboxyl stretch of the free carboxylic acid group for non-hydrogen-bonded COOH at 1700 cm^{-1}. Comparing the IR spectra of Fe_3O_4@Au MNPs and 16-MHA modified Fe_3O_4@Au MNPs, the absorption peaks caused by Fe_3O_4@Au MNPs were overlaid by those of 16-MHA. This information provided predominant evidence that the Fe_3O_4 core was coated by Au shell at high coverage and the following modification with 16-MHA was performed with high efficiency. Though the information provided by XRD and UV–vis spectra proved that the coated Au shell was not thick enough to exhibit much stronger signal to overlay that of the Fe_3O_4 core, the FT-IR spectra indicated that the Au shell of Fe_3O_4@Au MNPs was efficiently modified with 16-MHA via Au–S chemistry, taking advantages of both functional surface and smaller weight contribution to the decrease in the magnetic strength.

For protein conjugation, NHS and EDAC were employed for activating the carboxylic acid group of 16-MHA, which were self-assembled on the surface of Fe_3O_4@Au MNPs. This strategy was approved by using GFP as a model protein. As shown in Fig. S2A, GFP

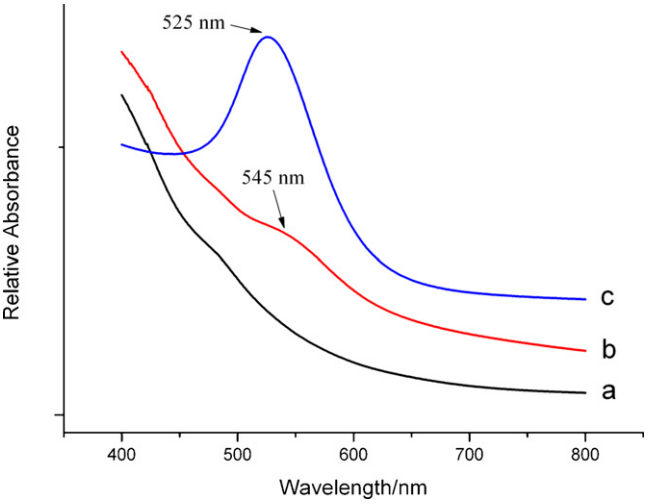

Fig. 6. UV–vis absorption spectra of Fe_3O_4 (a), Fe_3O_4@Au MNPs (b) and Au NPs (c) in water.

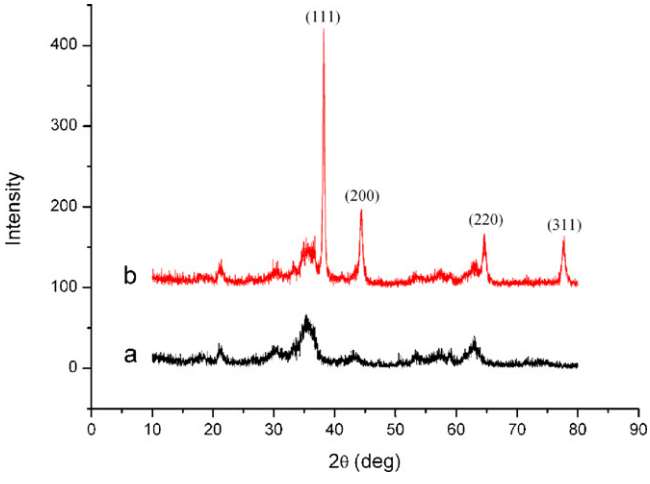

Fig. 5. X-ray powder diffractometer (XRD) for Fe_3O_4 (a) and Fe_3O_4@Au MNPs (b).

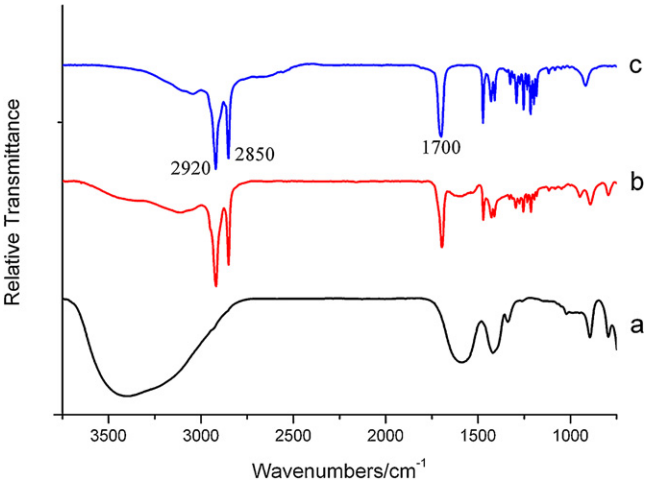

Fig. 7. FT-IR spectra of Fe_3O_4@Au (a), Fe_3O_4@Au@16-MHA MNPs (b) and pure 16-MHA (c).

Table 1
Comparison of efficiency on magnetic cell separation by using anti-CD3 modified Fe_3O_4@Au MNPs prepared via "non-oriented binding" and "oriented binding" strategy.

Cell amount for separation	Non-oriented binding			Oriented binding		
	Content of $CD3^+$ T cell (%)		Depletion efficiency (%)	Content of $CD3^+$ T cell (%)		Depletion efficiency (%)
	Before separation	After separation		Before separation	After separation	
1×10^6	59.3	27.4	53.8	36.5	1.5	95.9
2×10^6	59.3	32.9	44.5	36.5	0.7	98.1

conjugated Fe_3O_4@Au MNPs were visibly fluorescent under the epi-fluorescent microscope. It indicated that the NHS-EDAC catalyzed conjugation between carboxylated Fe_3O_4@Au MNPs and GFP was successful, which was applied for the direct covalent immobilization of anti-CD3 mAb.

Although direct covalent immobilization of antibody onto carboxylated magnetic nanoparticles is a common method, denaturation of some fraction of antibody might occur. And immobilized antibodies are always present in a random orientation on the surface (defined as "non-oriented binding"), with many molecules incapable of binding the target due to steric constraints or the blocking of binding sites, which might influence the coupling efficiency of antibody and antigen. Therefore, an "oriented binding" method for anti-CD3 mAb was carried out through covalently immobilizing protein A as the Fc receptor, followed by affinity capture of the antibody's Fc domains. The anti-CD3 mAb coated Fe_3O_4@Au MNPs were further characterized by SDS-PAGE. The immobilized anti-CD3 mAb was released from the magnetic nanoparticles by heating the SDS-PAGE loading buffer containing anti-CD3 mAb coated Fe_3O_4@Au MNPs in boiling water. As shown in Figure S2B, the loading buffer which was treated with anti-CD3 mAb coated Fe_3O_4@Au MNPs was loaded in Lane 2, and anti-CD3 mAb was loaded in Lane 1 as the control. Compared with Lane 1, anti-CD3 mAb was detected in Lane 2, indicating that anti-CD3 mAb was successfully conjugated to Fe_3O_4@Au MNPs through the "oriented binding" strategy.

The concentration of antibody was measured by Bradford protein assay, obtaining the calibration curve of absorbance at 595 nm versus antibody concentration (Fig. S3). By comparing the concentration of antibody before and after the coupling reaction, the amount of antibody immobilized on 1 mg Fe_3O_4@Au MNPs was estimated to be 120–135 μg in "non-oriented binding" strategy, and 60–65 μg in "oriented binding" strategy (measured 3 times).

3.3. Cell separation with anti-CD3 mAb modified Fe_3O_4@Au MNPs

Isolation or depletion of a certain kind of living cell from animal splenocytes with bioconjugated nanoparticles is one of important applications in biochemistry or immunology research. Depletion of $CD3^+$ T cells from whole splenocytes of mouse was carried out with anti-CD3 mAb modified Fe_3O_4@Au MNPs. The mouse splenocytes contain approximately 60–70% B cells and 30–40% $CD3^+$ T cells. The cell separation results using Fe_3O_4@Au MNPs modified with "non-oriented" and "oriented" anti-CD3 mAb were compared (Table 1). Although the conjugation capacity of anti-CD3 mAb on Fe_3O_4@Au MNPs by "non-oriented binding" was larger than that of "oriented binding", the cell depletion efficiency was on the contrary. The reason was that in the "non-oriented binding", anti-CD3 mAb was immobilized on the Fe_3O_4@Au MNPs in various orientations, and a relative high percentage of the recognition sites were blocked. However, the "oriented" bound anti-CD3 mAb left its Fab pointing away from the nanoparticle surface, allowing high antibody activity maintenance.

Table 2
Magnetic cell separation results of depleting $CD3^+$ T cell by using anti-CD3 modified Fe_3O_4@Au MNPs prepared via "oriented binding" strategy.

Cell amount for separation	Content of $CD3^+$ T cell (%)		Depletion efficiency (%)
	Before separation	After separation	
1×10^6	36.5	1.5	95.9
2×10^6	36.5	0.7	98.1
3×10^6	30.8	0.7	97.7
9×10^6	30.8	0.5	98.4

As shown in Fig. 8, for 9×10^6 whole splenocytes, the percentage of $CD3^+$ T cells which was 30.8% before depletion, decreased to 0.5% after depletion, with depletion efficiency of 98%. And the anti-CD3 mAb modified MNPs by "oriented binding" also had high efficiency on separating 1×10^6, 2×10^6 and 3×10^6 of mouse splenocytes. As shown in Table 2, 95.9–98.4% of $CD3^+$ T cell in whole splenocytes was depleted after magnetic cell separation. It indicated that the MNPs modified with oriented anti-CD3 mAb captured by protein A successfully stained $CD3^+$ T cells in the mixture of whole splenocytes.

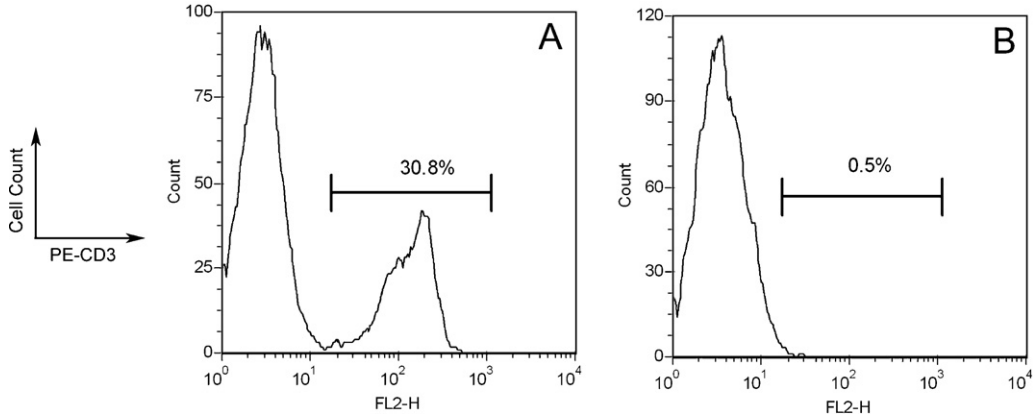

Fig. 8. The content of $CD3^+$ T cell in 9×10^6 whole splenocytes before (A) and after (B) magnetic cell separation analyzed by flow cytometry.

4. Conclusions

A simple, efficient and cost effective method for synthesizing anti-CD3 mAb immobilized Fe_3O_4@Au MNPs was developed for magnetic separation of whole splenocytes to deplete $CD3^+$ T cells. The synthesized core/shell Fe_3O_4@Au MNPs were characterized by XRD and UV–vis spectra, which confirmed that a thin Au shell was successfully coated on the Fe_3O_4 core. And the FT-IR data indicated that the Fe_3O_4 core was coated with the thin Au shell at high coverage because the absorption peaks of Fe_3O_4@Au MNPs were overlaid by the subsequently modified 16-MHA monolayer. The anti-CD3 mAb was immobilized on Fe_3O_4@Au MNPs via "oriented binding" strategy, in which protein A was introduced as the Fc receptor of the antibody. Fe_3O_4@Au MNPs immobilized with oriented anti-CD3 mAb were highly efficient in binding and depleting $CD3^+$ T cells from the whole splenocytes, and showed a higher level for antibody activity maintenance compared with those immobilized with non-oriented anti-CD3 mAb. Therefore, our bioconjugated Fe_3O_4@Au MNPs provide an efficient tool for the cell separation process and further present the dramatic potential to be applied to other areas of chemical and biological applications such as microextraction, immunoassay, biosensor and so on.

Acknowledgement

This work was supported by the National Natural Science Foundation of China (no. 30890142, 20975007, 20805002 and 90713013).

Appendix A. Supplementary data

Supplementary data associated with this article can be found, in the online version, at doi:10.1016/j.talanta.2011.05.010.

References

[1] J. Bao, W. Chen, T.T. Liu, Y.L. Zhu, P.Y. Jin, L.Y. Wang, J.F. Liu, Y.G. Wei, Y.D. Li, ACS Nano 1 (2007) 293–298.
[2] S.J. Guo, D. Li, L.M. Zhang, J. Li, E.K. Wang, Biomaterials 30 (2009) 1881–1889.
[3] Y. Liang, J.L. Gong, Y. Huang, Y. Zheng, J.H. Jiang, G.L. Shen, R.Q. Yu, Talanta 72 (2007) 443–449.
[4] Y.W. Jun, J.H. Lee, J. Cheon, Angew. Chem. Int. Ed. 47 (2008) 5122–5135.
[5] J.D. Qiu, M. Xiong, R.P. Liang, H.P. Peng, F. Liu, Biosens. Bioelectron. 24 (2009) 2649–2653.
[6] T.J. Zhang, W. Wang, D.Y. Zhang, X.X. Zhang, Y.R. Ma, Y.L. Zhou, L.M. Qi, Adv. Funct. Mater. 20 (2010) 1152–1160.
[7] T.T. Baby, S. Ramaprabhu, Talanta 80 (2010) 2016–2022.
[8] H.R. Zhang, M.E. Meyerhoff, Anal. Chem. 78 (2006) 609–616.
[9] Z.C. Xu, Y.L. Hou, S.H. Sun, J. Am. Chem. Soc. 129 (2007) 8698–8699.
[10] L.Y. Wang, J. Luo, Q. Fan, M. Suzuki, I.S. Suzuki, M.H. Engelhard, Y.H. Lin, N. Kim, J.Q. Wang, C.J. Zhong, J. Phys. Chem. B 109 (2005) 21593–21601.
[11] Y. Deng, D. Qi, C. Deng, X. Zhang, D. Zhao, J. Am. Chem. Soc. 130 (2008) 28–29.
[12] W.R. Zhao, J.L. Gu, L.X. Zhang, H.R. Chen, J.L. Shi, J. Am. Chem. Soc. 127 (2005) 8916–8917.
[13] J.C. Liu, P.J. Tsai, Y.C. Lee, Y.C. Chen, Anal. Chem. 80 (2008) 5425–5432.
[14] T.H. Ji, V.G. Lirtsman, Y. Avny, D. Davidov, Adv. Mater. 13 (2001) 1253–1256.
[15] X.Q. Liu, Y.P. Guan, Y. Yang, Z.Y. Ma, X.B. Wu, H.Z. Liu, J. Appl. Polym. Sci. 94 (2004) 2205–2211.
[16] J.L. Lyon, D.A. Fleming, M.B. Stone, P. Schiffer, M.E. Williams, Nano Lett. 4 (2004) 719–723.
[17] M.C. Daniel, D. Astruc, Chem. Rev. 104 (2004) 293–346.
[18] K.C. Grabar, R.G. Freeman, M.B. Hommer, M.J. Natan, Anal. Chem. 67 (1995) 735–743.
[19] X.L. Zhao, Y.Q. Cai, T. Wang, Y.L. Shi, G.B. Jiang, Anal. Chem. 80 (2008) 9091–9096.
[20] S. Qiu, L. Xu, Y.R. Cui, Q.P. Deng, W. Wang, H.X. Chen, X.X. Zhang, Talanta 81 (2010) 819–823.
[21] H. Deng, X.L. Li, Q. Peng, X. Wang, J.P. Chen, Y.D. Li, Angew. Chem. Int. Ed. 44 (2005) 2782–2785.
[22] H.L. Liu, C.H. Sonn, J.H. Wu, K.M. Lee, Y.K. Kim, Biomaterials 29 (2008) 4003–4011.
[23] S.H. Sun, H. Zeng, J. Am. Chem. Soc. 124 (2002) 8204–8205.
[24] H. Yu, M. Chen, P.M. Rice, S.X. Wang, R.L. White, S.H. Sun, Nano Lett. 5 (2005) 379–382.
[25] C.G. Wang, J. Chen, T. Talavage, J. Irudayaraj, Angew. Chem. Int. Ed. 48 (2009) 2759–2763.
[26] I.I.S. Lim, P.N. Njoki, H.Y. Park, X. Wang, L.Y. Wang, D. Mott, C.J. Zhong, Nanotechnology 19 (2008) 305102.
[27] G.K. Kouassi, J. Irudayaraj, Anal. Chem. 78 (2006) 3234–3241.
[28] J. Jeong, T.H. Ha, B.H. Chung, Anal. Chim. Acta 569 (2006) 203–209.
[29] H. Neubert, E.S. Jacoby, S.S. Bansal, R.K. Iles, D.A. Cowan, A.T. Kicman, Anal. Chem. 74 (2002) 3677–3683.
[30] H. Wang, Y.L. Liu, Y.H. Yang, T. Deng, G.L. Shen, R.Q. Yu, Anal. Biochem. 324 (2004) 219–226.
[31] M.M. Bradford, Anal. Biochem. 72 (1976) 248–254.
[32] U.K. Laemmli, Nature 227 (1970) 680–685.
[33] T.T.H. Pham, C. Cao, J. Sim, J. Magn. Magn. Mater. 320 (2008) 2049–2055.
[34] S. Laurent, D. Forge, M. Port, A. Roch, C. Robic, L.V. Elst, R.N. Muller, Chem. Rev. 108 (2008) 2064–2110.
[35] L. Babes, B. Denizot, G. Tanguy, J.J. Le Jeune, P. Jallet, J. Colloid Interface Sci. 212 (1999) 474–482.
[36] J.A. Creighton, D.G. Eadon, J. Chem. Soc.-Faraday Trans. 87 (1991) 3881–3891.